Ionic size and atomic disorder effects on the charge-density-wave transitions in $R_5Ir_4Si_{10}$(R=Dy-Lu)

Y. -K. Kuo,[1,*] F. H. Hsu,[2] H. H. Li,[2] H. L. Huang,[2] C. W. Huang,[2] C. S. Lue,[3] and H. D. Yang[2,†]
[1]*Department of Physics, National Dong Hwa University, Hualien 974, Taiwan*
[2]*Department of Physics, National Sun-Yat-Sen University, Kaohsiung 804,Taiwan*
[3]*Department of Physics, National Cheng Kung University, Tainan 701, Taiwan*
(Received 12 November 2002; revised manuscript received 14 February 2003; published 1 May 2003)

We report the systematic investigations of specific heat C, thermal conductivity κ, and thermoelectric power on the rare-earth–transition-metal ternary compounds $R_5Ir_4Si_{10}$(R = Dy, Ho, Er, Tm, Yb, and Lu) as a function of temperature. For all measured thermal properties, pronounced anomalous responses were observed near the charge-density-wave (CDW) transition temperature T_P in these compounds (except R=Yb). Particularly, the complex temperature-dependent thermal transport properties observed in these materials indicate very complicated heat transport processes during the phase transitions. Although these phase transitions can be associated with the CDW formation, the measured anomalies are considerably large, in contrast to those found in other weak-coupled CDW materials. In addition, it is found that T_P decreases linearly with the decreasing ionic radius of rare-earth elements from $Dy_5Ir_4Si_{10}$ to $Lu_5Ir_4Si_{10}$, but it increases nonlinearly with x in $(Lu_{1-x}Er_x)_5Ir_4Si_{10}$. These observations indicate that both ionic-size and atomic-disorder effects play important roles for the CDW transitions in this class of materials.

DOI: 10.1103/PhysRevB.67.195101 PACS number(s): 71.45.Lr, 71.20.Lp, 65.40.−b

I. INTRODUCTION

Ternary rare-earth–transition-metal silicides $R_5T_4Si_{10}$(R = rare-earth elements; T=Co, Ir, Rh, and Os), crystallized in the three-dimensional tetragonal $Sc_5Co_4Si_{10}$-type structure, have attracted considerable attention due to their variety of phase transitions. Especially, the interplay between superconductivity and long-range magnetic ordering at low temperatures (below 10 K) in these materials has been studied in detail.[1–15] High-temperature phase transitions attributed to the charge-density-wave (CDW) formation were also discovered in the $R_5T_4Si_{10}$ system.[3–8] The direct evidence of the CDW formation in this class of materials was not available until the successful growth of single crystals by Becker *et al.* and Galli *et al.*, with which the CDW superlattices in the x-ray diffraction were indeed observed in $Lu_5Ir_4Si_{10}$ and $Er_5Ir_4Si_{10}$.[16–18] The result of x-ray diffraction on the single crystal of $Er_5Ir_4Si_{10}$ has revealed the formation of an incommensurate CDW state at T_P = 155 K, which locks into a pure commensurate state below the incommensurate to the commensurate transition temperature T_0=55 K.[17] For $Lu_5Ir_4Si_{10}$, one CDW transition at T_P=80 K was found, and the experimental signature for the CDW ground state is associated with an incommensurate state below T_P.[16]

Our results of thermal measurements reported recently in $Lu_5Ir_4Si_{10}$ show that the anomalous responses at the CDW transitions (T_P~80 K) are rather unusual in the following ways:[19] (1) An extremely sharp transition with $\Delta T_P/T_P$ ~1% with no resolvable thermal hysteresis was found; (2) a quantitative specific-heat analysis for $Lu_5Ir_4Si_{10}$ near the fluctuation region yields a critical exponent α~2, much larger than the predicted mean-field value α=0.5; and (3) a giant excess thermal conductivity $\Delta\kappa/\kappa$~15% and a rapid change in the sign of thermoelectric power at T_P were observed.[19] However, similar studies on its isostructural compound $Lu_5Rh_4Si_{10}$ yield a different observation in some ways. For example, a clear thermal hysteresis (ΔT_P~5 K) in $Lu_5Rh_4Si_{10}$ was observed near its CDW transition T_P ~147 K by transport and thermodynamic measurements. No detectable magnetic-field (H) effect on the phase transition was found with H up to 8 T.[20,21]

To further understand the anomalous nature of the CDW transitions in this class of materials, we perform systematic investigations on the rare-earth–transition-metal ternary compounds $R_5Ir_4Si_{10}$ (R=Dy–Lu) near their CDW transitions. It is found that a sharp anomaly in C was observed in each compound (except R=Yb), ranging from T_P=210 K (Dy) to 80 K (Lu). However, multiple anomalies were observed in Dy, Ho, Er, and Tm by thermal transport measurements. By comparing the anomalous responses on these thermal properties, both normal-incommensurate (at T_P) and incommensurate-commensurate (at T_0) CDW transitions are expected to exist in these materials. Both T_P and T_0 decrease quasi-linearly with decreasing lattice parameter of rare-earth ions from Dy to Lu. In addition, T_P was found to increase nonlinearly with x in the $(Lu_{1-x}Er_x)_5Ir_4Si_{10}$ system. These observations indicate that both ionic-size and atomic-disorder effects play important roles for the CDW transitions in this class of materials.

II. EXPERIMENTAL METHODS

The preparation and characterization of polycrystalline $R_5Ir_4Si_{10}$ have been described elsewhere.[8] Briefly, samples were prepared by arc-melting stoichiometric mixtures of high-purity elements in a Zr-gettered argon atmosphere. The resulting ingots were turned and remelted at least five times to promote homogeneity. Samples were then sealed in quartz ampoules with about 160 Torr of argon and annealed at 1250°C for one day followed by three days at 1050°C.

Relative specific heats C were determined with a high-resolution ac calorimeter, using chopped light as a heat source. The absolute value of the specific heat for $Lu_5Ir_4Si_{10}$ has been determined by measuring a powder sample ($\sim$200 mg) using a differential scanning calorimetry, as described in detail in Ref. 19. The absolute values of $R_5Ir_4Si_{10}$ (R=Dy–Lu) are then assumed to be all equal at 300 K. Thermal conductivity κ and thermoelectric power (TEP) measurements were carried out simultaneously in a close-cycle refrigerator over temperatures ranging from 8 to 300 K, using a direct heat-pulse technique. The details of the measurement techniques can be found in Refs. 19–21.

At least two samples of each compound were measured to check experimental reproducibility. All presented features in this paper are reproducible for different experimental runs on the same sample, but the observed anomalies of each sample are slightly different from batch to batch with a variation less than 10%. We thus present results on the sample with the sharpest anomaly at T_P for each compound. In addition, all experiments were performed on both warming and cooling at a rate of 30 K/h to check any possible thermal hysteresis.

III. RESULTS AND DISCUSSION

A. Specific heat of $R_5Ir_4Si_{10}$ (R=Dy–Lu)

Measured temperature-dependent specific heats C for $R_5Ir_4Si_{10}$ (R=Dy–Lu) were illustrated in Fig. 1. In general, the observed specific heat C is a combination of lattice background and anomalous peaks. Clearly, one sharp peak in C was found in each compound (except R=Yb), ranging from T_P=210 K (Dy) to 80 K (Lu). T_P was determined from the temperature of the peak position, and the transition width ΔT_P was defined by the temperature width of half the peak height for each material. It is noted that T_P determined from C measurements are consistent with the previously reported temperature-dependent resistivity (ρ-T) results.[8] Since the observations of CDW superlattices from the x-ray diffraction in $Lu_5Ir_4Si_{10}$ and $Er_5Ir_4Si_{10}$ have been provided as the direct evidence of the CDW formations below T_P's,[16,17] the nature of these phase transitions found in the $R_5Ir_4Si_{10}$ system is presumably associated with the formation of a CDW.

The specific-heat jumps ΔC near the transitions in these materials can be estimated by subtracting a smooth lattice background of $Yb_5Ir_4Si_{10}$, which has no transition at high temperatures. The values of entropy change ΔS for other compounds are then obtained by integrating the curves under $\Delta C/T$ vs T with a temperature range covering the transition region. No thermal hysteresis near the phase transition is observed within the resolution limit of our apparatus. This is in contrast to that of its isostructural compound $Lu_5Rh_4Si_{10}$, in which pronounced thermal hysteresis loops between heating and cooling cycles have been observed in the vicinity of its CDW transition temperature $T_0\sim$147 K.[21] A summary regarding the characteristics of the specific-heat anomalies on $R_5Ir_4Si_{10}$ is tabulated in Table I. For comparison, we included the reported values for $Lu_5Ir_4Si_{10}$ in the table. Generally the sharpness of the transition $\Delta T_P/T_P\sim$1% (Lu)–2.4% (Dy) and excess specific-heat $\Delta C/C\sim$14% (Dy)–26% (Lu) were estimated for these materials. These values constitute the series compounds with the sharpest transition among all existing CDW materials ever reported. It is noted that the specific-heat jump and the entropy change at the transition in our polycrystalline $Lu_5Ir_4Si_{10}$ samples are somewhat smaller than those obtained from single crystals.[16] It is presumably due to this reason that these single crystals have a better sample quality than that of our polycrystalline samples, even though the transition width of our samples is close or even narrower than that presented by Becker and co-workers.

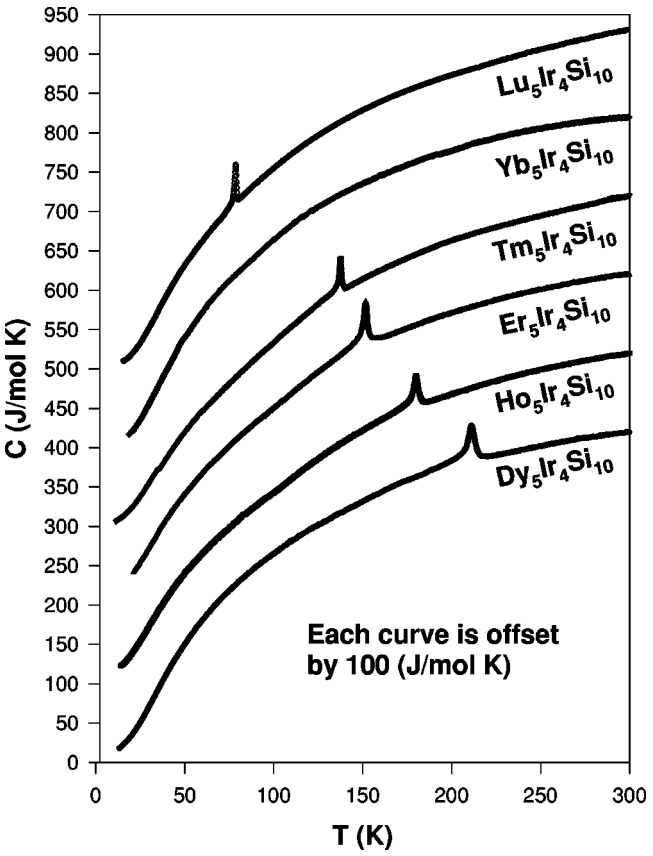

FIG. 1. The temperature dependence of specific heats for $R_5Ir_4Si_{10}$ (R=Dy–Lu). No thermal hysteresis was observed within the resolution limit of our apparatus.

For $Er_5Ir_4Si_{10}$, in addition to the spike-shaped peaks found near the CDW transition temperature T_P=152 K, a weaker secondary C anomaly (slope change) was detected in $Er_5Ir_4Si_{10}$ at 60 K, as demonstrated in Fig. 2(b). These results are consistent with those observed in resistivity measurements.[7,8] The x-ray diffraction on the single crystal $Er_5Ir_4Si_{10}$ has also confirmed the formation of an incommensurate CDW state at T_P=145 K, which locks into a purely commensurate state below T_0=55 K.[17]

For $Tm_5Ir_4Si_{10}$, two possible CDW transitions at T_P=138 K and T_P'=115 K, and two magnetic phase transitions at 0.86 and 1.91 K were reported previously.[8] For the upper two transitions, a sharp peak ($\Delta T_P/T_P\sim$1.1%) was found at T_P=138 K, while no noticeable anomaly was observed at T_P'=115 K in specific-heat measurements. However, as we will discuss in the following section, sharp anomalies were found in thermal conductivity and thermo-

TABLE I. Summary of specific-heat anomalies of the $R_5Ir_4Si_{10}$ system.

	T_P (K)	T_0 (K)	$\Delta T_P/T_P$ (%)	ΔC (J/mol K)	$\Delta C/C$(%)	ΔS (R)
$Dy_5Ir_4Si_{10}$	211.2	Undetectable	2.4	55	14	0.26
$Ho_5Ir_4Si_{10}$	180.0	Undetectable	1.7	40	13	0.16
$Er_5Ir_4Si_{10}$	151.8	60	2.0	60	18	0.38
$Tm_5Ir_4Si_{10}$	137.7	35	1.1	45	15	0.17
$Yb_5Ir_4Si_{10}$	48.0		Slope change	Slope change		
$Lu_5Ir_4Si_{10}$[a]	79.8		1.0	55	26	0.12

[a]Values are taken from Ref. 19.

electric power measurements at both 138 K and 115 K. It is possible that the anomalies found in transport measurements at T_P' is related to a second CDW transition that occurred in a different crystallographic direction, while only very little amount of entropy change is involved. The phase transition at 35 K observed in present C studies, as shown in the inset of Fig. 2(a), should arise from the same mechanism as that at $T_0 \sim 60$ K in $Er_5Ir_4Si_{10}$. Single-crystal x-ray diffraction measurements in this material are needed to confirm this point.

For $Yb_5Ir_4Si_{10}$, a small bump accompanied by a sudden slope change in C near 48 K was observed, while no visible anomalies at high temperatures were detected for this material. This observation is consistent with the transition feature found previously in resistivity measurements.[8] The transition temperature of $Yb_5Ir_4Si_{10}$ lies significantly below the linear depression of T_P for other compounds, as earlier reported in Ref. 8. This deviation was attributed to a valence fluctuation of Yb ions at low temperature. As a result, the ionic-size change is not as dominant as the electronic-configuration difference on the influence of the anomaly. This also explains that there are many different features between $Lu_5Ir_4Si_{10}$ and $Lu_5Rh_4Si_{10}$ though they have almost identical lattice parameters.

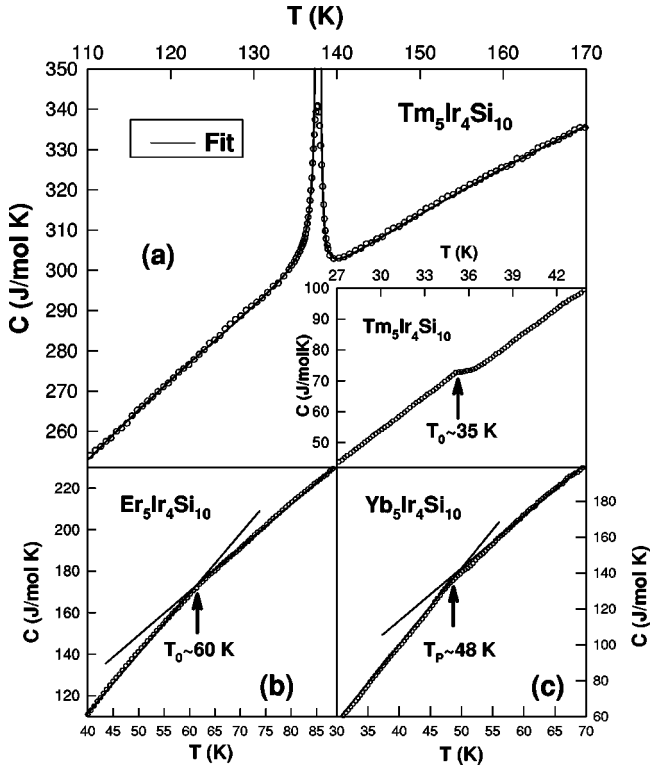

FIG. 2. (a) The agreement between the data points (open circles) and the fit (solid curve) in the vicinity of the CDW transition for $Tm_5Ir_4Si_{10}$. The inset shows the blow-up plot at low temperatures. (b) Low-temperature specific heat for $Er_5Ir_4Si_{10}$. A noticeable slope change is observed around 60 K. (c) A close-up $C-T$ plot for $Yb_5Ir_4Si_{10}$ near the transition. The straight lines are guides to the eyes.

The specific-heat data of $R_5Ir_4Si_{10}$ near the CDW transitions were analyzed via a least-squares-fitting procedure to a model of critical fluctuations in addition to the BCS mean-field contributions.[19] In this respect, the specific heat C consists of three terms

$$C = C_L + C_{MF} + C_{fl}, \tag{1}$$

where C_L is the lattice background, C_{MF} is the mean-field term below T_P, and C_{fl} is associated with fluctuation contributions. We assume that the lattice specific heat has the form of the Einstein model:

$$C_L = a_1\left(\frac{a_2}{T}\right)^{a_3}\frac{e^{a_2/T}}{(e^{a_2/T}-1)^2}. \tag{2}$$

The fitting functions are expressed as

$$C^- = C_L + \gamma^* T_P(1+\beta t) + b^-|t|^{-\alpha^-}, \quad T<T_P;$$

$$C^+ = C_L + b^+|t|^{-\alpha^+}, \quad T>T_P. \tag{3}$$

In Eq. (3), the mean-field term below T_P is represented by

$$C_{MF} = \gamma^* T_o(1+\beta t), \tag{4}$$

and the fluctuation part is

$$C_{fl}^- = b^-|t|^{-\alpha^-}, \quad T<T_P;$$

$$C_{fl}^+ = b^+|t|^{-\alpha^+}, \quad T>T_P. \tag{5}$$

Here a_1, a_2, a_3, γ^*, β, b^-, b^+, α^-, and α^+ are effective fitting parameters, where α^- and α^+ are known as critical exponents, and $t=(T_P-T)/T_P$ is the reduced temperature. The detailed fitting procedure was described in Ref. 19. In this work, a representative fitting result for $Tm_5Ir_4Si_{10}$ regarding Eq. (3) is shown in Fig. 2(a). A satisfactory agree-

TABLE II. Fitting parameters of the specific-heat of $R_5Ir_4Si_{10}$ to a model of critical fluctuations in addition to the mean-field contributions.

	Background term			Mean-field term		Fluctuations contribution			
	a_1(J/mol K)	a_2(K)	a_3	γ^* (J/mol K^2)	β	b^- (J/mol K)	α^-	b^+(J/mol K)	α^+
$Dy_5Ir_4Si_{10}$	409	205	1.82	2.0×10^{-2}	5.0	6×10^{-1}	0.8	2.6×10^{-2}	1.5
$Ho_5Ir_4Si_{10}$	417	224	1.80	8.5×10^{-3}	6.0	6.2×10^{-1}	0.8	4.7×10^{-3}	1.8
$Er_5Ir_4Si_{10}$	415	218	1.81	1.0×10^{-2}	4.0	14×10^{-1}	0.7	1.5×10^{-1}	1.1
$Tm_5Ir_4Si_{10}$	398	204	1.72	3.0×10^{-2}	6.0	6.5×10^{-1}	1.1	1.2×10^{-3}	1.8
$Lu_5Ir_4Si_{10}$[a]	306	115	1.46	7.7×10^{-2}	6.0	1.54×10^{-3}	1.8	4.8×10^{-4}	2

[a]Values are taken from Ref. 19.

ment between the fit and the measured data can be clearly seen. A similar quality of fitting results was also obtained for $Dy_5Ir_4Si_{10}$, $Ho_5Ir_4Si_{10}$, and $Er_5Ir_4Si_{10}$ (not shown here). The fitting parameters of specific heats of $R_5Ir_4Si_{10}$ with this model are listed in Table II. It is worthwhile mentioning that the critical exponents α^- and α^+ extracted from the best fit for these materials are larger than the value due to the Gaussian fluctuations with $\alpha^-=\alpha^+=0.5$, normally seen in typical CDW materials.[22–24] The higher powers of divergence in C near T_P' reflect very narrow transition widths in these materials. Besides, the coherence length ξ_0 of the order of 5 Å can be deduced for these compounds by using the Ginzburg criteria $\Delta T_G=(T_P/32)(k_B/\pi\Delta C_p\xi_o^3)^2$, $\Delta T_G \sim 10$ K is the temperature region where the fluctuations are important. Such a short coherence length seems to meet the criteria of McMillan's model proposed for the strong-coupled CDW systems,[25] an indication of the strong interchain couplings in $R_5Ir_4Si_{10}$. As a result, the spike-shape specific-heats near the CDW transitions and larger critical exponents extracted from the specific-heat fits can be attributed to the manifestation of strong interchain couplings in the studied compounds. This finding is similar to other CDW materials of 4.4 Å for $K_{0.3}MoO_3$ (Refs. 22 and 23) and 4.5 Å for 2H-$TaSe_2$ (Ref. 24). Besides, it was reported that the sharp specific jump in 2H-$TaSe_2$ is presumably due to the existence of a large number of soft phonon modes in the transition region, with which it provides a substantial specific-heat arising from their occupation.[24] This soft phonon mode scenario could also explain the origin of huge specific jumps exhibited in the titled system.

In Table II, it is noted that the important quantity γ^*, ranging from 8.5×10^{-3} J/mol K^2 (Ho) to 7.7×10^{-2} J/mol K^2 (Lu), was obtained from the fit. Here γ^*T_P, ranging from 1.53 J/mol K (Ho) to 6.16 J/mol K^2 (Lu), represents the electronic specific-heat jump of the mean-field term at the transition. The larger value of γ^*T_P for $Lu_5Ir_4Si_{10}$ is presumable due to a larger portion of the Fermi surface nesting in $Lu_5Ir_4Si_{10}$ as compared to other compounds. This is evident from the magnetic-susceptibility measurements in these materials,[3,8] in which $Lu_5Ir_4Si_{10}$ exhibits a more pronounced anomaly in χ at T_P, and in turn gives a larger change of the density of states associated with the CDW formation.

B. Thermal conductivity and thermoelectric power of $R_5Ir_4Si_{10}$ (R=Dy–Yb)

The temperature-dependent thermal conductivity κ and the TEP for $R_5Ir_4Si_{10}$ (R=Dy, Ho, Er, Tm, and Yb) are illustrated in Figs. 3–7. The values of room temperature κ for these compounds are between 80 mW/cm K (Dy) and 150 mW/cm K (Er), reasonable for their metallic nature. At low temperatures, κ increases with increasing temperature and a broad maximum appears at around 40 K for $R_5Ir_4Si_{10}$. This is a typical feature for the reduction of thermal scattering at

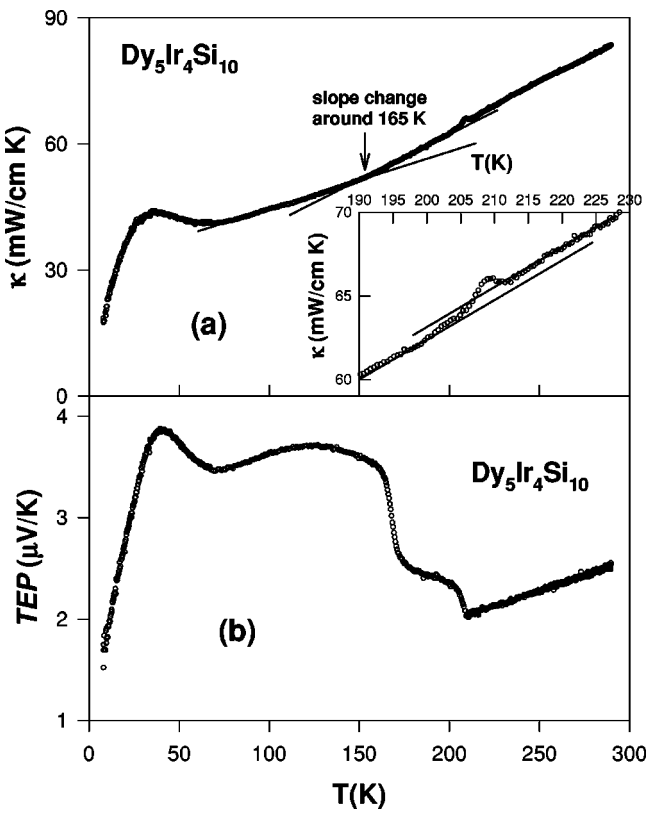

FIG. 3. (a) Thermal conductivity vs temperature of $Dy_5Ir_4Si_{10}$. A peak at 208 K and a slope change at 165 K are observed. The inset shows the details near the 208 K transition. (b) Thermoelectric power vs temperature for $Dy_5Ir_4Si_{10}$. Sharp increases are found at both 208 K and 165 K. The low-temperature maximum around 40 K is attributed to the phonon-drag effect.

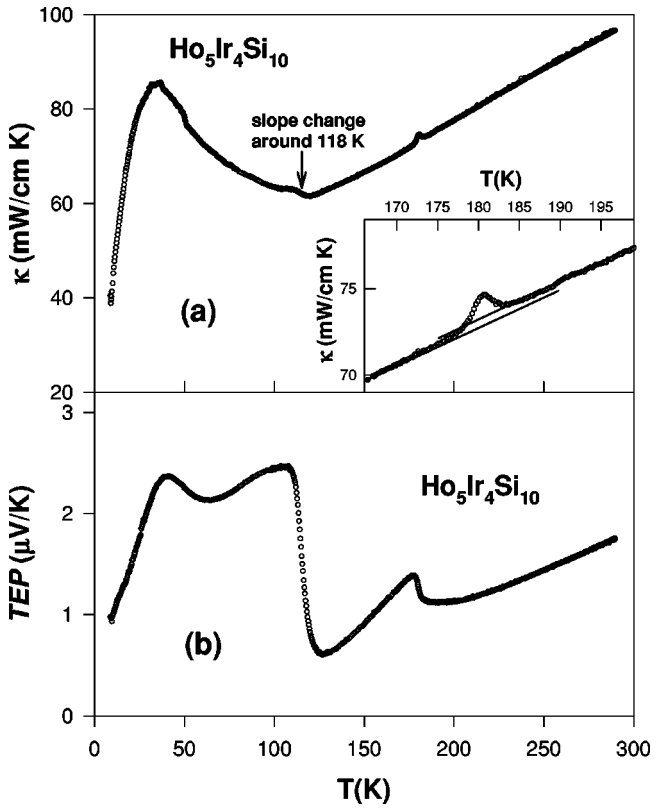

FIG. 4. (a) Thermal conductivity vs temperature of $Ho_5Ir_4Si_{10}$. A peak at 180 K and a slope change at 118 K are observed. The inset shows the details near the 180 K transition. (b) Thermoelectric power vs temperature for $Ho_5Ir_4Si_{10}$. Sharp increases are found at both 180 K and 118 K.

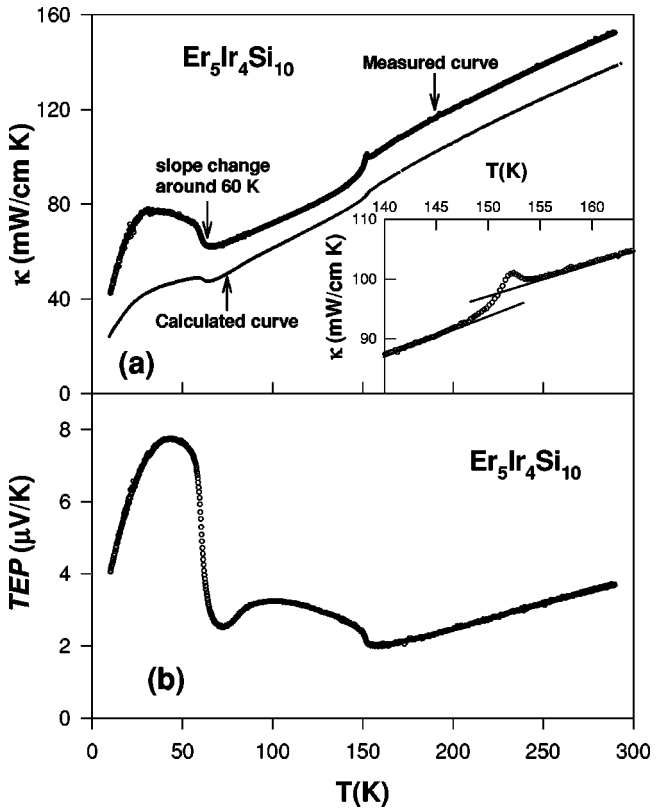

FIG. 5. (a) Thermal conductivity vs temperature of $Er_5Ir_4Si_{10}$. A peak at 152 K and a slope change at 60 K are observed. The dotted curves represent the combination of lattice and electronic contributions to κ_T. Note that the calculated results have been vertically shifted down by 20 mW/cm K for clarity. The inset shows the details near the 152-K transition. (b) Thermoelectric power vs temperature for $Er_5Ir_4Si_{10}$. Sharp increases are found at both 152 and 60 K.

lower temperatures for solids. Pronounced anomalies were found in thermal conductivity measurements (except Yb) in this system. The properties of the thermal conductivity anomalies for the $R_5Ir_4Si_{10}$ system were summarized in Table III. For the TEP results, the data in the normal state show a quasilinear behavior with positive slopes for all studied materials. The values of the TEP for $R_5Ir_4Si_{10}$ (R = Dy–Tm) are positive for the entire temperature range, signifying that hole-type carriers dominate their thermoelectric powers. On the other hand, $Yb_5Ir_4Si_{10}$ is an exception in this series with negative TEP, an indication of the electronlike carriers. Rapid changes on the thermoelectric power in the vicinity of phase transitions were seen. In the following, the details of the observed thermal transport features will be addressed case by case.

a. $Dy_5Ir_4Si_{10}$. As shown in Fig. 3, anomalies at 211 K were found by thermal conductivity and TEP measurements in $Dy_5Ir_4Si_{10}$. This phase transition was associated with the CDW formation, consistent with the observation in specific-heat measurements. The excess thermal conductivity $\Delta\kappa/\kappa \sim 2.7\%$ was estimated. In addition, thermal transport measurements show secondary anomalies at 165 K, as indicated by a slope change in κ and a sudden increase in TEP. However, there is no noticeable anomaly observed in C at this temperature.

b. $Ho_5Ir_4Si_{10}$. The anomalous features in $Ho_5Ir_4Si_{10}$ are very similar to those in $Dy_5Ir_4Si_{10}$ on thermal transport properties, as illustrated in Fig. 4. The corresponding T_P for this material is about 180 K, consistent with the value determined by the specific-heat. The excess thermal conductivity $\Delta\kappa/\kappa \sim 2.8\%$ was obtained. Secondary anomalies indicated by a slope change in κ and a sudden jump in TEP at 118 K were also found.

c. $Er_5Ir_4Si_{10}$. Sharp anomalies at around 152 K were observed by thermal transport measurements in $Er_5Ir_4Si_{10}$, as shown in Fig. 5. The anomaly at this temperature has been confirmed to be a commensurate CDW phase transition, according to the observation of the CDW superlattices from the x-ray diffraction in $Er_5Ir_4Si_{10}$ single crystals.[17] The excess thermal conductivity $\Delta\kappa/\kappa \sim 6.3\%$ was estimated. In addition, secondary anomalies accompanied by an abrupt slope change in κ and a sudden jump in TEP were discovered at 60 K for this compound.

d. $Tm_5Ir_4Si_{10}$. The compound of $Tm_5Ir_4Si_{10}$ exhibits very complicated thermal transport features, as shown in Fig. 6. The CDW phase transition occurs at $T_P = 138$ K, as indicated by a huge peak in κ with $\Delta\kappa/\kappa \sim 14\%$ and a clear maximum in TEP. In addition to the anomalies at T_P, we

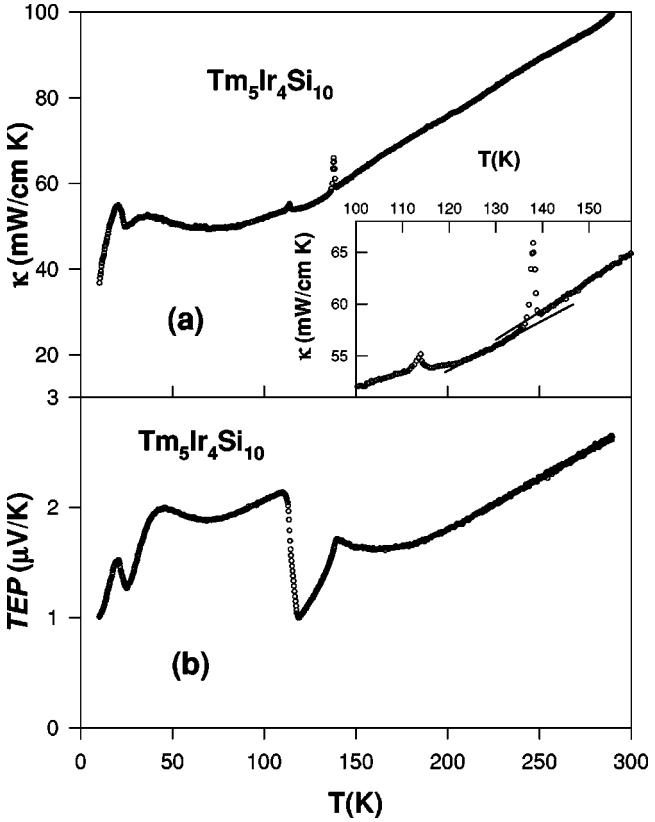

FIG. 6. (a) Thermal conductivity vs temperature of $Tm_5Ir_4Si_{10}$. Three sharp peaks are observed at 138 K, 113 K, and 21 K, respectively. (b) Thermoelectric power vs temperature for $Tm_5Ir_4Si_{10}$.

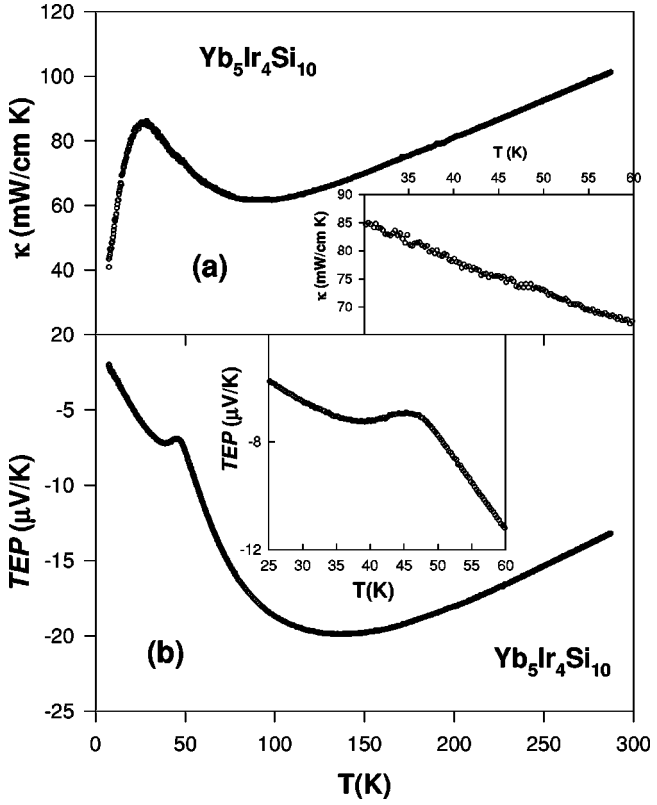

FIG. 7. (a) Thermal conductivity vs temperature of $Yb_5Ir_4Si_{10}$. No noticeable anomaly in κ is observed. (b) Thermoelectric power vs temperature for $Yb_5Ir_4Si_{10}$. A kink in TEP is observed around 48 K.

also observed a smaller peak ($\Delta\kappa/\kappa\sim 3\%$) in κ and an abrupt increase in TEP at 113 K, in spite of the absence of the specific-heat anomaly at this temperature. Besides, well-defined peaks are found in κ and TEP for $Tm_5Ir_4Si_{10}$ at 20.5 K (peaks position), which is 15 K lower than the anomaly found in C.

e. $Yb_5Ir_4Si_{10}$. $Yb_5Ir_4Si_{10}$ exhibits exceptional behaviors in thermal transport properties, as compared to other compounds in this series. A kink-shaped anomaly at $T_P=48$ K in TEP was observed, as shown in Fig. 7(b). However, there is no noticeable anomaly in κ at this temperature [Fig. 7(a)], within the resolution of our apparatus. Besides, the absolute values of TEP at 300 K for $Yb_5Ir_4Si_{10}$ ($|\mathrm{TEP}|\sim 15\mu$ V/K) is about an order of magnitude larger than that of $R_5Ir_4Si_{10}$ with $R=$ Dy–Tm($|\mathrm{TEP}|\sim 2$). Most interestingly, the sign of TEP for $Yb_5Ir_4Si_{10}$ is negative, in contrast to the positive TEP values for other compounds in the temperature range we measured. Such a result suggests that the dominant carriers for the thermal transport in $Yb_5Ir_4Si_{10}$ have an opposite character than that of all other members in $R_5Ir_4Si_{10}$.

Now we discuss the features of thermal transport properties in the studied compounds. Due to the metallic nature of these compounds, the total thermal conductivity κ_T can be expressed as a sum of lattice (κ_L), electronic (κ_e), and anomalous terms ($\Delta\kappa$):

$$\kappa_T=\kappa_L+\kappa_e+\Delta\kappa. \tag{6}$$

The lattice part κ_L is expected to follow $1/T$ behavior, while the electronic contribution κ_e can be determined by

TABLE III. Summary of thermal conductivity anomalies of the $R_5Ir_4Si_{10}$ system.

	T_P (K)	$\Delta\kappa_P/\kappa_P$ (%)	T_0 (K)	$\Delta\kappa_0/\kappa_0$ (%)
$Dy_5Ir_4Si_{10}$	211	2.7	165	Slope change
$Ho_5Ir_4Si_{10}$	180	2.8	118	Slope change
$Er_5Ir_4Si_{10}$	152	6.3	60	Slope change
$Tm_5Ir_4Si_{10}$	$T_P=138$, $T_P'=113$	14(T_P), 2.8(T_P')	21	12
$Yb_5Ir_4Si_{10}$	Undetectable			
$Lu_5Ir_4Si_{10}$[a]	80	15		

[a]Values are taken from Ref. 19.

means of the Wiedmann-Franz law: $\kappa_e\rho/T=L_o$. Here, ρ is the dc electrical resistivity and the Lorentz number $L_o=2.45\times10^{-8}$ WΩ K^{-2}. It was suggested previously that the significant reduction in κ at the transition is mainly due to the deficiency of conduction electrons, and the anomalous change in κ has essentially an electronic origin in $Lu_5Ir_4Si_{10}$.[19] This scenario is also perfectly applicable in the $Er_5Ir_4Si_{10}$ case, where a reduction in κ at 152 K and an increase at 60 K correspond well to the increase and reduction in ρ at these phase transitions. The result of detailed calculations of Eq. (6) to the measured κ for $Er_5Ir_4Si_{10}$ is plotted in Fig. 5(a). The thin line represents the calculated κ for $Er_5Ir_4Si_{10}$, in good agreement with the observed result except near the anomalous peak. This analysis provides a clear confirmation that the anomalous κ changes in these materials are of electronic origin. However, the appearance of giant $\Delta\kappa$ (for examples, $\Delta\kappa/\kappa\sim14\%$ for $Tm_5Ir_4Si_{10}$ at 138 K and 15% for $Lu_5Ir_4Si_{10}$ at 80 K) cannot be simply explained by changes in electron-or phonon-scattering processes at the transitions. Such anomalies in thermal conductivity were also observed in $K_{0.3}MoO_3$ and $(TaSe_4)_2I$ at the CDW transitions, but with much broader and smaller peaks. Kwok and co-workers associated the peak (5%) in κ with the specific-heat jump (6%) in $K_{0.3}MoO_3$ as a result of heat carried by the soft phonon and mode occupation.[26] Since the softening modes near $2k_F$ are propagating, the heat carried by the soft phonons is considerable and is responsible for the giant $\Delta\kappa$. Hence, both C and κ features around T_P could be qualitatively understood in terms of this picture.

Another common feature of the thermal conductivity in the studied compounds is their high-temperature variation. In the normal state ($T>T_P$), the κ data increase monotonically with temperature for all compounds. Such a behavior has also been found in $K_{0.3}MoO_3$ and $(TaSe_4)_2I$ (Ref. 26), which was attributed to the quasiparticle scattering due to fluctuations, and in turn gives a linear increase in κ at higher temperatures.[27] Consequently, a large number of soft Kohn-Peierls phonons would contribute to the high-temperature thermal conductivity. In fact, the lack of linear increase in κ at high temperatures in their isostructural compound $Sc_5Ir_4Si_{10}$ (with no CDW formation) further supports that the high-temperature variation in κ in these compounds is related to the CDW formation and due to the quasiparticle excitations.[28]

For the TEP measurements, rapid changes of TEP in the vicinity of transitions are generally observed in these materials (except $Yb_5Ir_4Si_{10}$). Since the TEP measurement is a sensitive probe of energy relative to the Fermi surface, the rapid changes of TEP in $R_5Ir_4Si_{10}$ are attributed to the sudden change of the band structure, associated with the electron-hole asymmetry at the transitions. In the normal state ($T>T_P$), the TEP varies rather linearly with temperature in these materials. Thus, one can try to extract the value of E_F through the classical formula $S=\pi^2k_B^2T/2eE_F$, assuming a one-band model with an energy-independent relaxation time. The values of E_F between 2.7 eV (Er) and 5.9 eV (Dy) for $R_5Ir_4Si_{10}$ were obtained from this simple model. Note that this value represents a lower limit, because other effects such as the CDW fluctuations could contribute to additional high-temperature TEP with a linear temperature variation. However, this estimate is in good agreement with the metallic nature of these compounds. A summary regarding the characteristics of the TEP properties for $R_5Ir_4Si_{10}$ (R=Dy–Lu) is tabulated in Table IV.

TABLE IV. Summary of thermoelectric power anomalies of the $R_5Ir_4Si_{10}$ system.

	T_P (K)	T_0 (K)	E_F (eV)	Temperature range fitted (K)
$Dy_5Ir_4Si_{10}$	208	165	5.9	$210<T<300$
$Ho_5Ir_4Si_{10}$	180	118	4.7	$210<T<300$
$Er_5Ir_4Si_{10}$	152	60	2.7	$160<T<300$
$Tm_5Ir_4Si_{10}$	138	21	3.8	$200<T<300$
$Yb_5Ir_4Si_{10}$	48		0.7	$220<T<300$
$Lu_5Ir_4Si_{10}$[a]	80		2.2	$100<T<300$

[a]Values are taken from Ref. 19.

Finally, one could deduce the possible nature of the multiple phase transitions found in these materials by comparing the anomalous responses on their thermal properties. The high-temperature anomalies found at T_P in $R_5Ir_4Si_{10}$ ($T_P=211$ K for R=Dy, 180 K for Ho, 152 K for Er, and 138 K for Tm) are most likely due to the normal-incommensurate CDW formation, while the anomalies found at lower temperatures ($T_0=165$ K for R=Dy, 118 K for Ho, 60 K for Er, and 21 K for Tm) are the incommensurate-commensurate lock-in transition. The common features of the anomalies at the lock-in transition in these materials are that only weak (or no) anomalous responses in their specific-heats but sharp increases in their thermoelectric powers are observed. If it is the case, both T_P and T_0 have a linear depression with de-

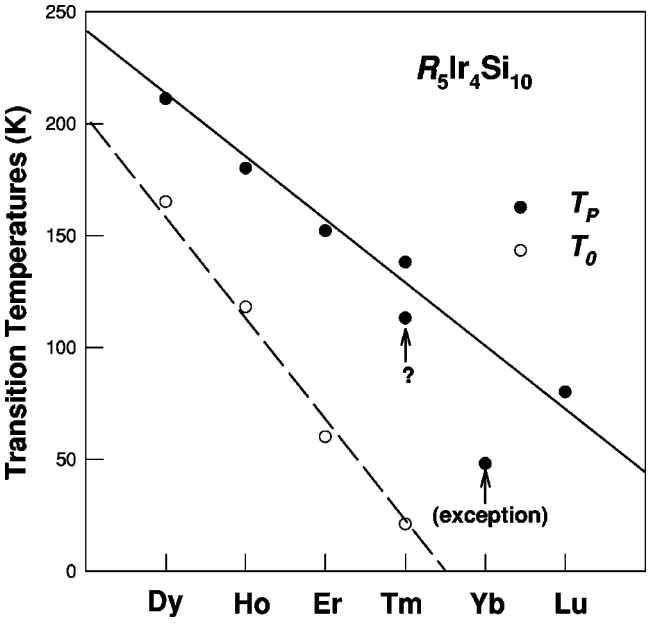

FIG. 8. The transition temperatures T_P (close circles) and T_0 (open circles) for $R_5Ir_4Si_{10}$ (R=Dy–Lu). Apparently, $Yb_5Ir_4Si_{10}$ is an exception in this series. Notice that this figure is in agreement with Fig. 4 of Ref. 8.

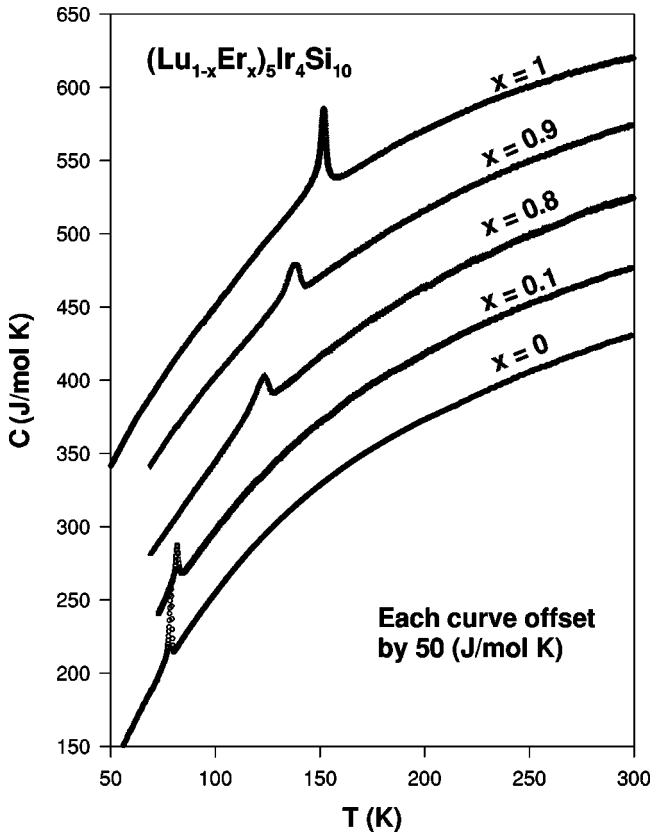

FIG. 9. The temperature dependence of specific-heats for $(Lu_{1-x}Er_x)_5Ir_4Si_{10}$.

creasing lattice parameters with rare-earth ions from Dy to Lu (except Yb), as shown in the Fig. 8. The anomaly observed in $Tm_5Ir_4Si_{10}$ at 113 K is probably a second CDW transition that occurred in a different crystallographic direction. Nevertheless, direct evidences such as single-crystal x-ray diffraction or neutron-scattering measurements are needed to clarify this scenario.

C. Thermal properties of $(Lu_{1-x}Er_x)_5Ir_4Si_{10}$

The temperature-dependent specific-heats of the substituted system $(Lu_{1-x}Er_x)_5Ir_4Si_{10}$ ($x=0$, 0.1, 0.8, 0.9, and 1.0) are illustrated in Fig. 9. We note that the T_P determined by present C measurements are consistent with the previously reported T-dependent resistivity (ρ-T) results.[8] After subtracting a smooth background, estimated by fitting a lattice background through the data far from the transition, we can obtain the specific heat jumps ΔC, entropy changes ΔS, and an excess specific heat $\Delta C/C$ at the transitions. A summary regarding the characteristics of the specific-heat anomalies for these alloys is listed in Table V. It is clearly seen that the excess specific heat $\Delta C/C$ at T_P is suppressed, and the transition width $\Delta T_P/T_P$ is broadened by the Er substitutions for Lu. Besides, it has been reported previously that the Fermi-level density of states of $Lu_5Ir_4Si_{10}$ is very sensitive to both external pressure[2] and internal pressure (impurity effects).[6] If one plots T_P (K), $\Delta T_P/T_P$ (%), and $\Delta C/C$ (%) vs x for $(Lu_{1-x}Er_x)_5Ir_4Si_{10}$ (see Fig. 10), a pronounced deviation from Vegard's law is clear seen. In this respect, the effects of both atomic disorder and internal pressure, introduced by substituting Er, for Lu play important roles for the CDW transitions found in the $(Lu_{1-x}Er_x)_5Ir_4Si_{10}$ system.

TABLE V. Summary of specific-heat anomalies of the $(Lu_{1-x}Er_x)_5Ir_4Si_{10}$ system.

	T_P (K)	$\Delta T_P/T_P$ (%)	ΔC (J/mol K)	$\Delta C/C$(%)	ΔS (R)
$x=0.00$[a]	79.8	1.0	55	26.0	0.12
$x=0.10$	81.6	2.0	26	11.1	0.10
$x=0.80$	122.5	6.5	21	7.0	0.23
$x=0.90$	137.4	5.5	22	6.6	0.18
$x=1.00$	151.8	2.0	60	18.0	0.38

[a]Values are taken from Ref. 19.

The T-dependent κ and TEP of $(Lu_{1-x}Er_x)_5Ir_4Si_{10}$ are illustrated in Figs. 11 and 12, respectively. According to our experimental uncertainty, the values of κ for $(Lu_{1-x}Er_x)_5Ir_4Si_{10}$ alloys are essentially unaffected with various x, except the anomalous features near phase transitions. In the normal state ($T>T_P$), κ rises monotonically with temperature, tending to a linear variation for all compositions. Such a peculiar behavior has been discussed in the preceding section. Anomalies were also found in thermal conductivity measurements in these alloys. For $x=0$, 0.1, and 1, a jump accompanied with a sharp peak in κ was observed at T_P in each compound. For $x=0.8$ and $x=0.9$,

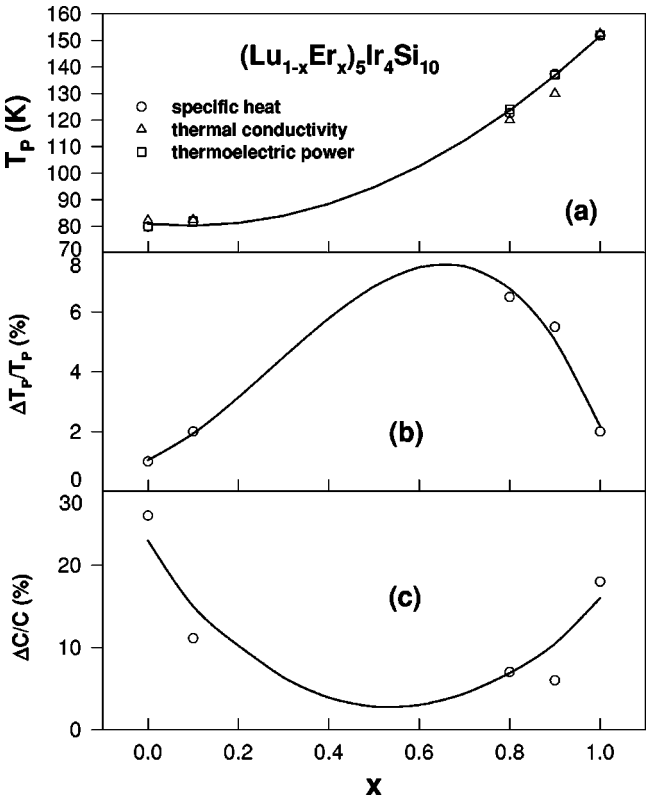

FIG. 10. T_P (K), $\Delta T_P/T_P$ (%), and $\Delta C/C$ (%) vs x in $(Lu_{1-x}Er_x)_5Ir_4Si_{10}$. The lines are guides to the eyes.

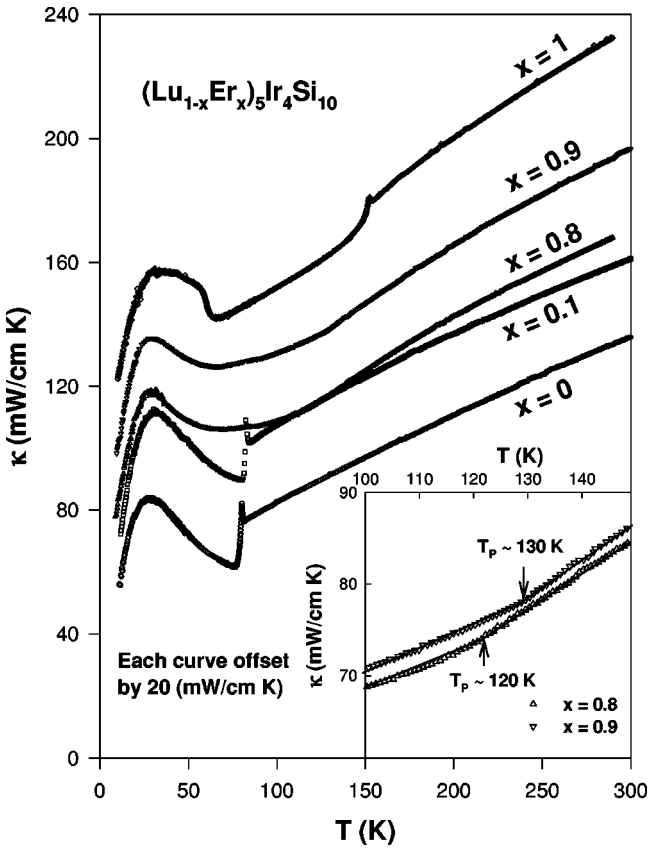

FIG. 11. Thermal conductivity vs temperature for $(Lu_{1-x}Er_x)_5Ir_4Si_{10}$. Inset: slope changes in κ were found at about 120 K and 130 K for $x = 0.8$ (up triangles) and $x = 0.9$ (down triangles), respectively.

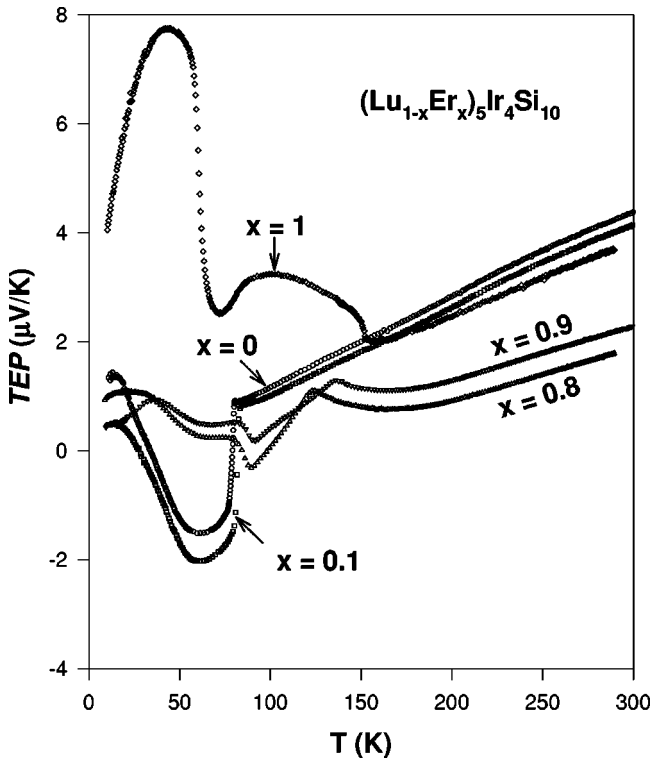

FIG. 12. TEP vs temperature for $(Lu_{1-x}Er_x)_5Ir_4Si_{10}$.

however, milder slope changes in κ were found at about 120 K and 130 K (see inset of Fig. 11), respectively, somewhat lower than what were observed in specific-heat measurements. The excess thermal conductivity $\Delta\kappa/\kappa \sim 15\%$ ($x=0$), 13% ($x=0.1$), and 6.3% ($x=1$) at T_P' are estimated. It has been discussed previously that the significant reduction in κ at transition is mainly due to the deficiency of conduction carriers, and the anomalous change in κ is essentially of electronic origin. For $x=0.8$ and $x=0.9$, only milder slope changes in κ were found at their CDW transitions. This observation is expected as weaker resistivity anomalies they exhibit.[8]

The *T*-dependent TEP exhibits the most complex features among all measured physical properties in $(Lu_{1-x}Er_x)_5Ir_4Si_{10}$. The values of TEP are positive in the normal state, signifying that hole-type carriers dominate their thermoelectric powers in these alloys. Generally, rapid changes in the thermoelectric power in the vicinity of phase transitions are observed. For $x=0$ and $x=0.1$, the TEP changes sign from positive values above T_P' to negative values below T_P', indicating a change of conduction mechanism or dominant carrier at transitions. For $x=1$, a minor increase at $T_P=152$ K and an even larger increase in TEP at 60 K were observed. Notice that resistivity measurements also reveal two sharp transitions on single-crystal $Er_5Ir_4Si_{10}$ at $T_P=155$ K, and $T_0=55$ K, respectively.[17] Anomalies in TEP were found at about 124 K and 137 K for $x=0.8$ and $x=0.9$, respectively, and kinks around 90 K were also observed for both compounds. The origin for these extra anomalies found in TEP is not understood at this moment and warrants further investigations. A summary regarding the characteristics of thermal transport anomalies for the $(Lu_{1-x}Er_x)_5Ir_4Si_{10}$ system was listed in Table VI.

Finally, it would be instructive to study the correlations among superconductivity (SC), magnetic order (MO), and the CDW formation in this $R_5Ir_4Si_{10}$ series using our previous and present data. It is preseted as follows.

(1) There is not one single pure compound in $R_5Ir_4Si_{10}$ (R=Dy–Lu, Y, and Sc) exhibiting both SC and MO, indicating that the SC and MO are strongly correlated and mutually incompatible, just as what we commonly understood.

(2) The SC ($T_C \sim 3.5$ K) and CDW ($T_P \sim 80$ K) coexist in the single pure compound $Lu_5Ir_4Si_{10}$. However, it is reminded that an interplay between SC and CDW was found in

TABLE VI. Summary of thermal transport anomalies of the $(Lu_{1-x}Er_x)_5Ir_4Si_{10}$ system.

	T_P (K) (taken from κ)	$\Delta\kappa_P/\kappa_P$ (%)	T_P (K) (taken from TEP)	E_F (eV)
$x=0.00$[a]	80.2	15.0	80	2.2
$x=0.10$	82.4	12.8	82	2.4
$x=0.80$	120.0	Slope change	124	3.6
$x=0.90$	130.0	Slope change	137	2.7
$x=1.00$	152.5	6.3	152	2.7

[a]Values are taken from Ref. 19.

$(Lu_{1-x}Sc_x)_5Ir_4Si_{10}$ (Ref. 7) and external pressure effects were observed in $Lu_5Ir_4Si_{10}$.[3] Thus, the SC and the CDW compete for the density of states in the Fermi surface, and in turn the SC and CDW suppress each other.

(3) T_N found in $R_5Ir_4Si_{10}$ (R=Dy–Tm) basically follows the scale of de Genne's relation, suggesting that the Ruderman-Kittel-Kasuya-Yosida interactions dominate the magnetism between the magnetic rare-earth ions.[8] Our previous results also show that T_P of $Tm_5Ir_4Si_{10}$ was suppressed by an external pressure, but its T_N was not.[8] In addition, T_P for $R_5Ir_4Si_{10}$ (R=Dy–Lu) depends linearly on the ionic radius of rare-earth elements, no matter R is magnetic or not. This implies that the MO at low temperature correlates insignificantly with the CDW in this $R_5Ir_4Si_{10}$ system.

IV. CONCLUSIONS

Thermal properties including specific-heat, thermal conductivity, and thermoelectric power in the rare-earth–transition-metal ternary compounds $R_5Ir_4Si_{10}$ (R=Dy–Yb) were studied in details. Generally, pronounced anomalous responses in their thermal properties are observed near the charge-density-wave transitions. The observed spike-shape specific heats near the CDW transitions and larger critical exponents extracted from the specific-heat fits can be attributed to the manifestation of strong interchain couplings in $R_5Ir_4Si_{10}$. By comparing the anomalous responses on the thermal properties in $R_5Ir_4Si_{10}$, both normal-incommensurate and incommensurate-commensurate CDW transitions are expected to exist in these materials. Besides, both T_P and T_0 decrease quasilinearly with the decreasing ionic radius of rare-earth ions from Dy to Lu. It is also found that T_P (K), $\Delta T_P/T_P$ (%), and $\Delta C/C$ (%) depend nonlinearly on x in $(Lu_{1-x}Er_x)_5Ir_4Si_{10}$. These observations indicate that the effects of ionic size and atomic disorder play important roles for the CDW transitions in this class of materials. In addition, our results suggest that the superconductivity and magnetic order are strongly correlated and mutually incompatible, the superconductivity and the CDW suppress each other, and the magnetic order at low temperature correlates insignificantly with the CDW in this $R_5Ir_4Si_{10}$ system.

ACKNOWLEDGMENTS

This work was supported by National Science Council, Taiwan under Grant Nos. NSC-91-2112-M-259-015 (Y.K.K.), NSC-91-2112-M-006-033 (C.S.L.), and NSC-91-2112-M-110-005 (H.D.Y.).

*Corresponding author. Email address: ykkuo@mail.ndhu.edu.tw
†Corresponding author.
Email address: yang@mail.phys.nsysu.edu.tw

[1] O. Fischer and M.B. Maple, *Superconductivity in Ternary Compounds* (Springer-Verlag, Berlin, 1984), Vol. II.
[2] H.D. Yang, R.N. Shelton, and H.F. Braun, Phys. Rev. B **33**, 5062 (1986).
[3] R.N. Shelton, L.S. Hausermann-Berg, P. Klavins, H.D. Yang, M.S. Anderson, and C.A. Swenson, Phys. Rev. B **34**, 4590 (1986).
[4] L.S. Hausermann-Berg and R.N. Shelton, Phys. Rev. B **35**, 6659 (1987).
[5] C.A. Swenson, R.N. Shelton, P. Klavins, and H.D. Yang, Phys. Rev. B **43**, 7668 (1991).
[6] H.D. Yang, P. Klavins, and R.N. Shelton, Phys. Rev. B **43**, 7676 (1991).
[7] H.D. Yang, P. Klavins, and R.N. Shelton, Phys. Rev. B **43**, 7681 (1991).
[8] H.D. Yang, P. Klavins, and R.N. Shelton, Phys. Rev. B **43**, 7688 (1991).
[9] S. Ramakrishnan, K. Ghosh, and Girish Chandra, Phys. Rev. B **45**, 10 769 (1992).
[10] S. Ramakrishnan, K. Ghosh, and Girish Chandra, Phys. Rev. B **46**, 2958 (1992).
[11] K. Ghosh, S. Ramakrishnan, and G. Chandra, Phys. Rev. B **48**, 10 440 (1993).
[12] K. Ghosh, S. Ramakrishnan, Arvind D. Chinchure, K. Jonason, V.R. Marathe, G. Chandra, and S.S. Shah, Phys. Rev. B **51**, 11 656 (1995).
[13] N.G. Patil and S. Ramakrishnan, Phys. Rev. B **56**, 3360 (1997).
[14] N.G. Patil and S. Ramakrishnan, Phys. Rev. B **59**, 9581 (1999).
[15] N.G. Patil and S. Ramakrishnan, B. Becker, A.A. Menovsky, and J.A. Mydosh, J. Appl. Phys. **85**, 4845 (1999).
[16] B. Becker, N.G. Patil, S. Ramakrishnan, A.A. Menovsky, G.J. Nieuwenhuys, and J.A. Mydosh, Phys. Rev. B **59**, 7266 (1999).
[17] F. Galli, S. Ramakrishnan, T. Taniguchi, G.J. Nieuwenhuys, J.A. Mydosh, S. Geupel, J. Ludecke, and S. van Smaalen, Phys. Rev. Lett. **85**, 158 (2000).
[18] F. Galli, R. Feyerherm, R.W. Hendrikx, S. Ramakrishnan, G.J. Nieuwenhuys, and J.A. Mydosh, Phys. Rev. B **62**, 13 840 (2000).
[19] Y.-K. Kuo, C.S. Lue, F.H. Hsu, H.H. Li, and H.D. Yang, Phys. Rev. B **64**, 125124 (2001).
[20] C.S. Lue, F.H. Hsu, H.H. Li, H.D. Yang, and Y.K. Kuo, Physica C **364-365**, 243 (2001).
[21] C.S. Lue, Y.K. Kuo, F.H. Hsu, H.H. Li, H.D. Yang, P. Fodor, and L.E. Wenger, Phys. Rev. B **66**, 033101 (2002).
[22] J.W. Brill, M. Chung, Y.-K. Kuo, X. Zhan, and E. Figueroa, Phys. Rev. Lett. **74**, 1182 (1995).
[23] M. Chung, Y.-K. Kuo, X. Zhang, E. Figueroa, J.W. Brill, and G. Mozurkewich, Synth. Met. **71**, 1891 (1995).
[24] R.A. Craven and S.F. Meyer, Phys. Rev. B **16**, 4583 (1977).
[25] W.L. McMillan, Phys. Rev. B **16**, 643 (1977).
[26] R.S. Kwok and S.E. Brown, Phys. Rev. Lett. **63**, 895 (1989).
[27] Kazumi Maki, Phys. Rev. B **46**, 7219 (1992).
[28] Y.K. Kuo, Y.-T. Pan, C.S. Lue, and H.D. Yang, J. Low Temp. Phys. **131**, 311 (2003).